Cell, Vol. 101, 555–567, May 26, 2000, Copyright ©2000 by Cell Press

The *SHORT-ROOT* Gene Controls Radial Patterning of the *Arabidopsis* Root through Radial Signaling

Yrjo Helariutta,*§‖ Hidehiro Fukaki,*§
Joanna Wysocka-Diller,*# Keiji Nakajima,*
Jee Jung,* Giovanni Sena,*
Marie-Theres Hauser,† and Philip N. Benfey*‡
*Department of Biology
New York University
1009 Main Building
New York, New York 10003
†Center of Applied Genetics
Universitaet fuer Bodenkultur Wien
Muthgasse 18
A-1190 Vienna
Austria

Summary

Asymmetric cell divisions play an important role in the establishment and propagation of the cellular pattern of plant tissues. The *SHORT-ROOT* (*SHR*) gene is required for the asymmetric cell division responsible for formation of ground tissue (endodermis and cortex) as well as specification of endodermis in the *Arabidopsis* root. We show that *SHR* encodes a putative transcription factor with homology to SCARECROW (SCR). From analyses of gene expression and cell identity in genetically stable and unstable alleles of *shr*, we conclude that SHR functions upstream of *SCR* and participates in a radial signaling pathway. Consistent with a regulatory role in radial patterning, ectopic expression of *SHR* results in supernumerary cell divisions and abnormal cell specification in the root meristem.

Introduction

Radial pattern formation in the *Arabidopsis* root is the result of highly regulated cell division and cell specification events. A well-characterized example is the ground tissue that originates from a set of stem cells ("initials") that undergo asymmetric cell divisions to give rise to the youngest cells of the endodermis and cortex cell lineages (Figure 1A). Subsequently, cells in both lineages undergo differential expansion resulting in cell types with distinct morphologies and differentiated features.

We have previously identified two loci, *SHORT-ROOT* (*SHR*) and *SCARECROW* (*SCR*), that control ground tissue patterning during root development in *Arabidopsis* (Benfey et al., 1993; Scheres et al., 1995). Mutations in these loci result in a single ground tissue layer, indicating that both loci are essential for the periclinal asymmetric cell division that gives rise to the two distinct cell files. In *scr* mutants, the remaining layer has differentiated attributes of both endodermis and cortex, indicating that *SCR* is essential for cell division but not differentiation of the ground tissue (Scheres et al., 1995; Di Laurenzio et al., 1996). In contrast to *scr*, the single layer of ground tissue in *shr* mutants is missing endodermal differentiation markers, indicating that SHR is essential for both cell division and cell specification (Benfey et al., 1993).

Because radial pattern defects in *shr* and *scr* are already evident during embryogenesis, it has been proposed that the radial pattern of the root is established during the formation of the embryonic root. The pattern is then propagated by the meristematic initial cells by a "top-down" signaling process moving from older to younger cells (Scheres et al., 1995). Further evidence for cell signaling in ground tissue formation has come from cell ablation studies. If the immediate daughter cells of three adjacent initial cells are ablated, the cell lineage corresponding to the central initial cell stops dividing periclinally (van den Berg et al., 1995). This implies the existence of signals for radial patterning of the ground tissue that are moving down, and perhaps to some degree laterally, in a single cell layer of the ground tissue. To date, very little is known about the molecular mechanisms of these signaling processes.

We report the isolation of the *SHR* gene that encodes a member of the GRAS family of putative transcription factors. The first member of this family to be identified was *SCR* (Di Laurenzio et al., 1996). The *SCR* gene is expressed in the initial daughter cell before its asymmetric division and remains expressed in the endodermal cell layer after the division (Di Laurenzio et al., 1996; Wysocka-Diller et al., 2000). We present evidence that SHR is necessary for the maintenance of *SCR* expression, indicating that SHR is upstream of *SCR*. Surprisingly, *SHR* RNA is not expressed in the ground tissue cell lineage but in the stele (pericycle and vascular cylinder) located immediately adjacent to it, suggesting a non-cell-autonomous mode of action of SHR. Ectopic expression of *SHR* results in supernumerary cell divisions and altered cell specification, indicating that SHR is both necessary and sufficient to regulate cell division and cell specification in the root meristem.

Results

SHORT-ROOT Is Required for Asymmetric Cell Division and Cell Specification in Ground Tissue

Previous analysis of two *shr* alleles (*shr-1* and *shr-2*) had shown that there is only a single cell layer between the epidermis and the pericycle of primary and secondary roots (Figure 1D) as compared to the normal radial organization of two ground tissue layers, cortex and endodermis (Figure 1C) (Benfey et al., 1993; Scheres et al., 1995). Two additional alleles (*shr-3* and *shr-4*) were identified in a screen of *Arabidopsis* lines containing the

‡To whom correspondence should be addressed (e-mail: philip.benfey@nyu.edu).
§These authors contributed equally to this work.
‖Present address: Plant Molecular Biology Laboratory, Institute of Biotechnology, POB 56 FIN00014, University of Helsinki, Finland.
#Present address: Department of Botany and Microbiology, Auburn University, Auburn, Alabama 36849.

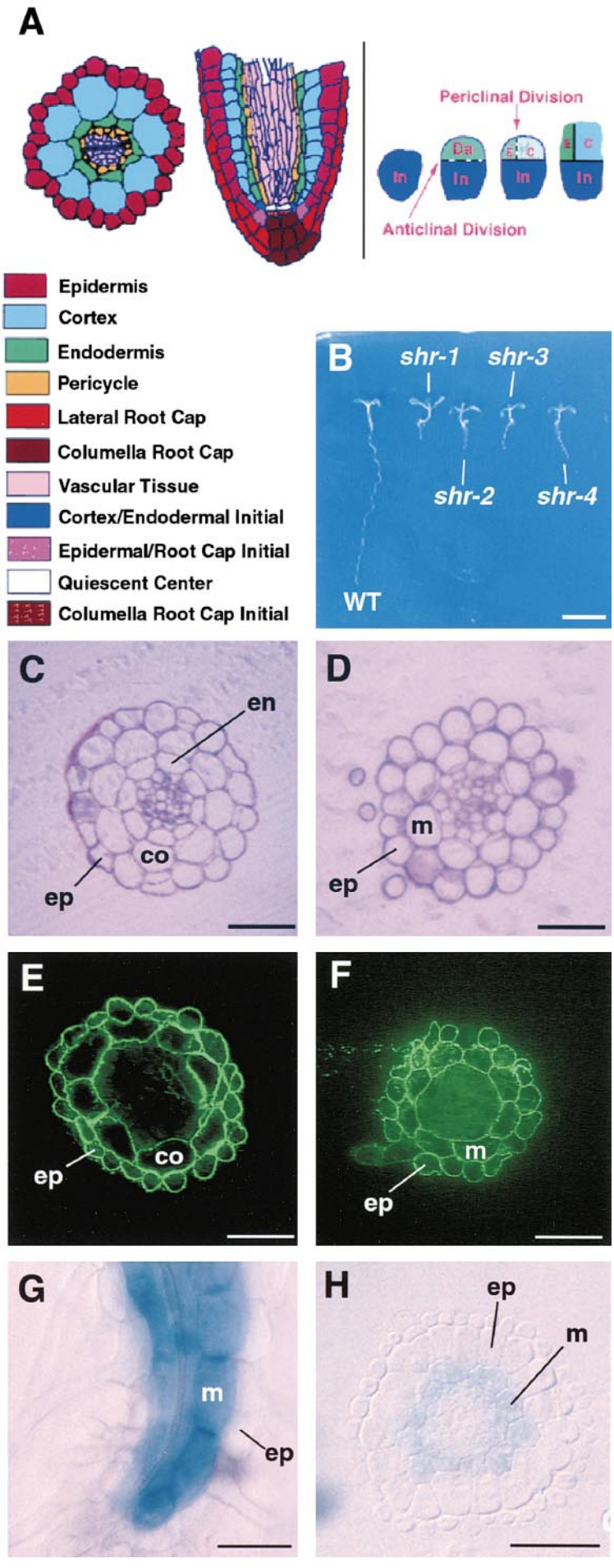

Figure 1. Phenotype of *shr* Mutant Plants

(A) Schematic of *Arabidopsis* root anatomy (left). Transverse section showing epidermis, cortex, endodermis, and pericycle surrounding the vascular tissue. In the longitudinal section, the epidermal/lateral root cap initials and the cortex/endodermal initials are shown at the base of their respective cell files. Schematic of division pattern of the cortex/endodermal initial (right). The initial expands and then divides anticlinally to reproduce itself and a daughter cell. The daughter then divides periclinally to produce the progenitors of the endodermis and cortex cell lineages. C, cortex; Da, daughter cell; E, endodermis; and In, initial. Similar schematics were in Di Laurenzio et al. (1996).

(B) 12-day-old wild-type (WT), *shr-1*, *shr-2*, *shr-3*, and *shr-4* seedlings grown vertically on nutrient agar medium. Transverse plastic sections of primary root of (C) wild-type and (D) *shr-2*. CCRC-M2 antibody staining in (E) epidermis and cortex of wild-type and in (F) epidermis and mutant layer of *shr-1* primary roots. *AX92::GUS* expression in mutant layer of (G) a longitudinal optical section and (H) a transverse section of a *shr-1* primary root. ep, epidermis; co, cortex; en, endodermis; and m, mutant ground tissue layer in *shr*. Bar, 10 mm (A) and 50 μm (B-H).

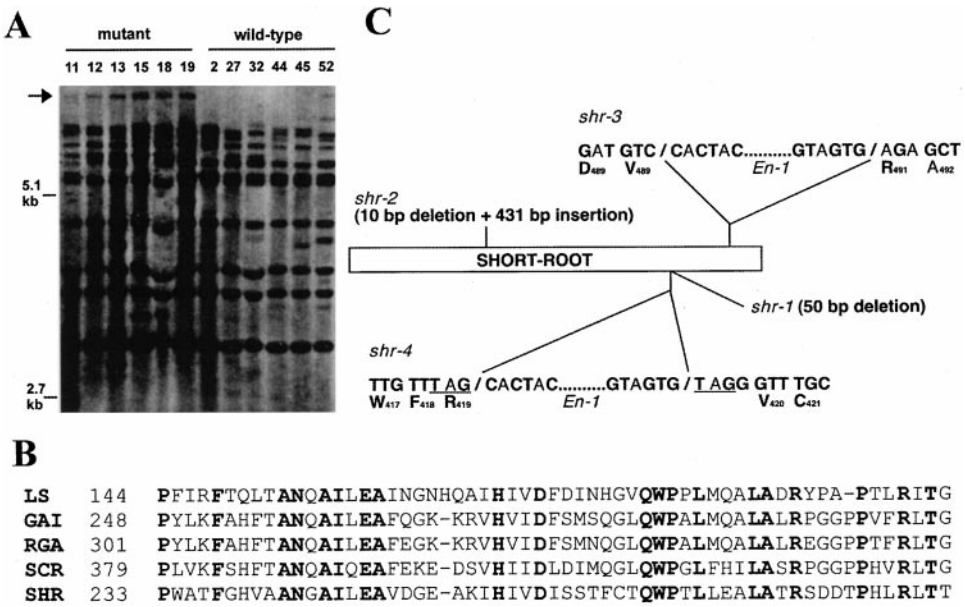

Figure 2. Molecular Cloning of the *SHR* Gene

(A) The candidate band of En hybridization cosegregating with the *shr* mutant phenotype is indicated (arrow). A band of similar size is found in one of the homozygous wild-type plants (line 52). PCR analysis of the En-*SHR* junction in this line indicated that the similar molecular weight band does not correspond to the band observed in the mutants. Numbers above the gel lanes indicate individual plants of the segregating population. Molecular size markers are indicated on the left.

(B) Alignment of the deduced amino acid sequence of the "VHIID domains" of five functionally characterized GRAS family genes (*Ls*: Schumacher et al., 1999; *GAI*: Peng et al., 1997; *RGA*: Silverstone et al., 1998; and *SCR*: Di Laurenzio et al., 1996). Numbers before the sequence indicate the position of the first amino acid of the alignment in the corresponding position in the proteins. Conserved amino acids are shown in bold. *SHR* is not highly similar to any other functionally characterized GRAS gene.

(C) Mutation sites in *shr* alleles. Note that *shr-4* has a duplication of nucleotide triplets (TAG; underlined) at the En insertion site, while the En insertion in *shr-3* did not result in an alteration of the host sequence.

autonomous maize En transposon (Wisman et al., 1998). All four alleles have a similar phenotype—seedlings have highly reduced root growth and darker cotyledons as compared to wild-type (Figure 1B) (with the exception of some *shr-3* and *shr-4* roots that contain revertant sectors).

Longitudinal optical sections indicate the presence of a cell at the normal position of the cortex/endodermal initial and no evidence for a periclinal division occurring in its immediate progeny (compare WT and *shr* in Figures 3D, 3G, 5B, and 5C). This indicates that a primary defect in *shr* is disruption of this asymmetric cell division.

To gain insight into the role of SHR in regulating cell specification, we determined the identity of the single mutant ground tissue cell layer present in *shr* roots. We had previously shown that two endodermal markers, production of the Casparian strip, and binding of the JIM13 antibody (Knox et al., 1990) do not occur in the mutant layer in *shr-1* (Benfey et al., 1993; Scheres et al., 1995) (compare WT and *shr* in Figures 7B and 7D). Here, we analyzed the status of two markers normally expressed in the cortex. The CCRC-M2 antibody binds to a carbohydrate epitope in the cell walls of epidermis and cortex (Di Laurenzio et al., 1996; Freshour et al., 1996). In *shr-1*, antibody staining is detected in the epidermis as well as the mutant ground tissue layer (compare WT and *shr* in Figures 1E and 1F). We further tested expression of an *AX92::GUS* construct that is specifically expressed in the root cortex (Dietrich et al., 1992; Malamy and Benfey, 1997). In *shr-1*, this construct expresses exclusively in the mutant layer (Figures 1G and 1H). These results indicate that the *shr* mutant layer has attributes of cortex and suggest that *SHR* is necessary for the specification of endodermis cell identity.

Transposon Tagging and Molecular Cloning of *SHR*

The *shr-3* and *shr-4* alleles segregated a variable number (5%–15%) of seedlings with a wild-type appearance suggesting excision of an En element from the *SHR* locus. Analysis of the progeny of several putative revertants indicated segregation ratios close to the expected 3:1 (wild-type to mutant), consistent with these being heterozygotes (data not shown). These two alleles were derived from lines that typically harbor more than ten copies of the En transposon (Wisman et al., 1998). To identify which En element was inserted into the *SHR* locus, a cosegregation analysis was carried out. A candidate band present in all mutants was identified (Figure 2A). Inverse PCR amplification was used to identify plant sequences flanking the candidate En element. Comparison to the databases revealed identity to a BAC-end sequence (see the Experimental Procedures).

Sequence analysis of the BAC revealed an ORF whose deduced amino acid sequence has significant homology to GRAS family genes (Figure 2B; Pysh et al., 1999). To verify the identity of the cloned gene, this region was amplified from *shr-1* and *shr-2* and sequenced. In *shr-1*, a deletion of 50 bp toward the 3′ end of the ORF results in a frameshift and premature termination of translation of the putative amino acid sequence (Figure 2C). In *shr-2*, there is a deletion of 10 bp followed by an insertion

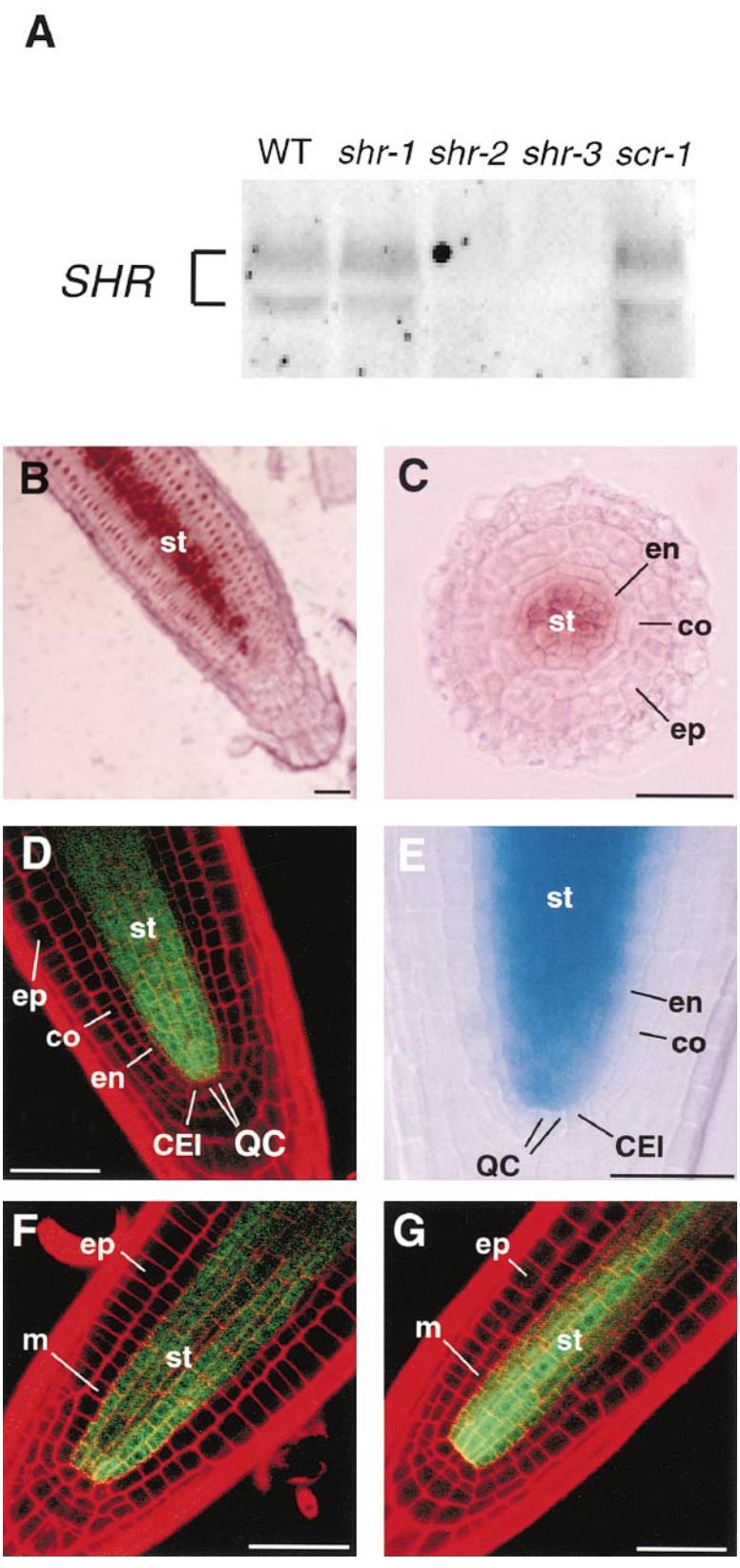

Figure 3. *SHR* Expression in the Primary Root

(A) *SHR* RNA accumulation in seedlings. Northern blot analysis was performed with total RNA from 12-day-old root tissues hybridized with a *SHR* gene-specific probe. Lanes are as marked. Levels of ribosomal RNA indicated approximately equal loading of all lanes (data not shown).

(B and C) In situ RNA hybridization with a *SHR* gene-specific probe. (B) Longitudinal and (C) transverse sections of wild-type primary roots hybridized with a digoxigenin-labeled antisense *SHR* gene-specific probe. Sense probes showed low-level nonspecific staining (data not shown). Longitudinal optical sections of wild-type roots with (D) confocal laser scanning microscopy of *SHR::GFP* or (E) histochemical staining (0.5 hr) of *SHR::GUS* reveal *SHR* expression in the stele tissue, not in the ground tissue lineage. Confocal images of *SHR::GFP* expression in (F) *scr-3* and (G) *shr-1* primary roots. Abbreviations as above except CEI, cortex/endodermal initial; QC, quiescent center; and st, stele. Bar, 50 μm.

of 431 bp (sequence that is identical to a moderately repetitive sequence) toward the 5′ end of the ORF (Figure 2C). This alteration in the DNA sequence would lead to premature termination of the putative peptide. The sites of insertion of the En elements in *shr-3* and *shr-4* were also determined (Figure 2C).

Further support for the identity of the cloned gene was obtained by analysis of the segregation of the *shr* locus-specific En element in the cloned gene in a population of plants representing progeny of a revertant. Excision of the En element cosegregated with the wild-type phenotype, and no other En elements cosegregated with the mutation (data not shown). The nature of the molecular defects and the identical phenotype of the four alleles indicates that they are likely to represent the null phenotype.

The protein encoded by the *SHR* locus would be 531 amino acids in length. All of the motifs found in SCR and the other members of the GRAS gene family (Pysh et al., 1999) are present in SHR. Unlike *SCR*, there do not appear to be any introns in the *SHR* locus.

SHR Is Expressed in Stele Tissue

RNA blot analysis revealed two transcripts in wild-type seedlings (Figure 3A, lane 1). The basis for the two transcripts was investigated by isolation and sequencing of two species of *SHR* cDNA. The only difference between the two species was in their 3′ UTRs in which one species' polyA tail was 109 bp further downstream than the other. Analysis of the 3′ genomic UTRs revealed two putative polyadenylation signals positioned 239 and 118 bp downstream of the putative termination codon. RT-PCR on either shoot or root tissue confirmed the presence of these two RNA species (data not shown). These results indicate that the two bands in the RNA blot probably represent transcripts with different polyadenylation sites although we cannot rule out additional factors, such as different lengths of the polyA tails.

SHR expression was analyzed in three *shr* alleles. The *shr-1* allele has the same level of *SHR* RNA as wild-type (Figure 3A). Transcript levels are severely reduced but still detectable in *shr-2* (Figure 3A). In *shr-3*, no transcripts were detected (Figure 3A), which may be the result of the large insertion by the En transposon.

To determine the spatial pattern of *SHR* expression, RNA in situ hybridization analysis was performed. By in situ hybridization, expression in the root appeared to be primarily in the stele, which comprises the central vascular cylinder and the surrounding pericycle (Figures 3B and 3C). To determine if the localization of *SHR* RNA was regulated at the transcriptional or posttranscriptional level, we fused 2.5 kb of 5′ upstream sequence to either the Green Fluorescent Protein (GFP) coding region (Haseloff et al., 1997) or to the GUS coding region. The *SHR* promoter region conferred expression that was restricted to the stele and extends down to the vascular initial cells (Figures 3D and 3E). No *SHR* expression was ever observed in the ground tissue cell lineage of the root, suggesting that *SHR* controls radial organization of ground tissue in a non-cell-autonomous manner.

Endodermis and cortex are first formed by an asymmetric cell division of the embryonic ground tissue (Scheres et al., 1995). In our previous study, we found that the *shr* mutation results in an absence of this asymmetric cell division (Scheres et al., 1995). We made use of the *SHR::GFP* reporter construct to characterize *SHR* expression at various stages of embryogenesis.

At the late globular stage, *SHR::GFP* is expressed in procambium cells in the lower tier, which is presumptive stele tissue (Figure 4A). At this stage, *SCR* is expressed in the ground tissue and hypophysis (Wysocka-Diller et al., 2000). At the triangular stage, *SHR::GFP* expression is observed in the procambium (Figure 4B). *SCR* expression at this stage is in the adjacent ground tissue and presumptive quiescent center cells (Wysocka-Diller et al., 2000). *SHR::GFP* expression in the procambium/stele is consistently observed at later stages of embryogenesis (Figure 4C, heart stage; Figure 4D, torpedo stages, Figures 4E and 4F, mature embryo). In addition, this expression extends into the cotyledon petiole, in the region of the presumptive cotyledon procambium (Figures 4D and 4F). No *SHR* expression was ever observed in the ground tissue cell lineage or presumptive quiescent center cells, consistent with the hypothesis that *SHR* controls radial organization of ground tissue in a non-cell-autonomous manner during embryogenesis.

SHR Is a Positive Regulator of *SCR* Expression

Both *SHR* and *SCR* regulate the asymmetric cell division of the endodermis/cortex initial daughter cell and of the embryonic ground tissue. *SHR* regulates both cell division and endodermis specification, whereas *SCR* appears to regulate primarily the cell division process. We hypothesized that *SHR* might be an upstream regulator of *SCR* in a pathway that results in asymmetric cell division. As an initial test of this hypothesis, double mutants were generated and found to have a phenotype identical to *shr-1* (data not shown). The epistasis of *shr* is consistent with our hypothesis and argues against a pathway in which *SCR* would be upstream of *SHR*.

To determine the relationship between SCR and SHR activity, we first examined the effect of the *scr* mutation on *SHR* expression. From RNA blot analysis, the level of *SHR* expression appears to be unaffected by the putative null *scr-1* mutation (Figure 3A, lane 5), indicating that *SHR* expression is not dependent on SCR activity. To investigate the spatial distribution of *SHR* expression in *scr* mutant roots, the *SHR::GFP* transgene was crossed into *scr-3*. In *scr-3* roots, *SHR::GFP* expression was still confined to the stele (Figure 3F), indicating that the establishment of the *SHR* expression pattern is not dependent on SCR activity. These results are consistent with the observation that the mutant ground tissue layer in *scr* retains endodermal differentiation attributes (Di Laurenzio et al., 1996).

To investigate the possibility that there might be a regulatory relationship at the transcriptional level with SHR upstream of *SCR*, an RNA blot analysis of *SCR* expression was performed in the *shr* background (Figure 5A). The consistently reduced expression of *SCR* in the *shr* mutant background indicates that SHR is essential for normal levels of *SCR* expression in the root. To investigate the spatial distribution of the remaining *SCR* expression in *shr* roots, a *SCR::GFP* transgene (Wysocka-Diller et al., 2000) was crossed into *shr*. In all *shr* alleles

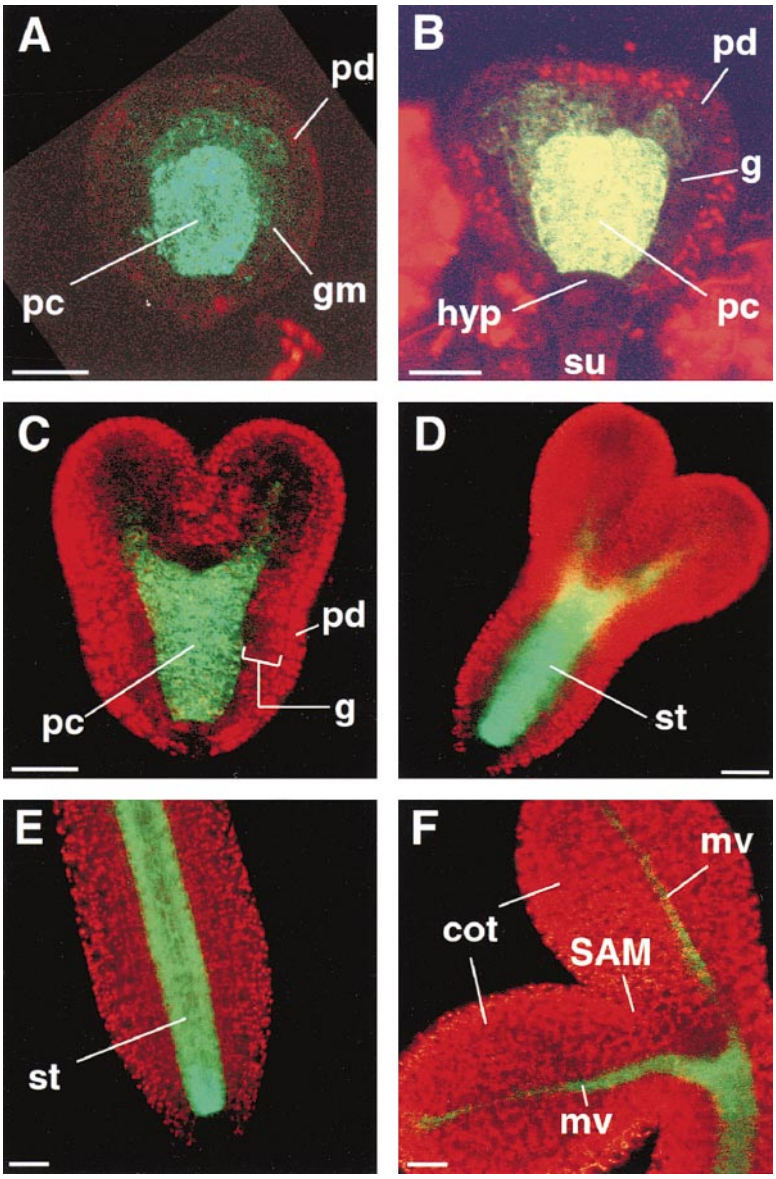

Figure 4. *SHR* Expression during Embryogenesis

Longitudinal view of *SHR::GFP* expression during wild-type embryogenesis. (A) Late globular stage; (B) triangular stage; (C) heart stage; (D) torpedo stage; (E) mature embryonic root; and (F) mature embryonic shoot. Abbreviations as above except cot, cotyledon; hyp, hypophysis; g, ground tissue; gm, ground meristem; mv, mid vein of cotyledon; pc, procambium; pd, protoderm; SAM, shoot apical meristem; and su, suspensor. Bar, 25 μm.

analyzed, the level of GFP expression was dramatically lowered compared to that in wild-type (compare Figures 5B and 5C). Faint expression in the single ground tissue layer and sometimes in the epidermal layer was observable near the meristematic region. No expression was detected in more differentiated tissue. We conclude that SHR is essential for maintenance of *SCR* expression in the promeristem and in more differentiated root cells. The residual level of *SCR* expression detected in the *shr* mutant ground tissue is apparently not sufficient for the correct radial patterning of the ground tissue.

To determine if SHR is involved in an autoregulation pathway, we examined the effect of the *shr* mutation on *SHR* expression using *shr-1* plants containing the *SHR::GFP* transgene. In these plants, expression was still restricted to the stele tissue (Figure 3G), indicating that SHR activity is not necessary for the transcriptional regulation of *SHR*.

Ectopic SHR Expression Alters Cell Division and Cell Specification

To determine if SHR is sufficient for cell division and cell specification when ectopically expressed, we placed the *SHR* coding region under the control of the Cauliflower Mosaic Virus (CaMV) 35S promoter, which is constitutively active in most plant tissues (Odell et al., 1985). Analysis of five independent transformants revealed supernumerary cell layers (from three to seven layers) surrounding the stele in the seedling root (Figures 6A and 6B). The number of extra layers varied among the different independent lines and among progeny from a single line, and the radial pattern was not always symmetric in the root (data not shown). In all lines, the stele appeared similar to wild-type. In longitudinal optical sections, it appeared that the additional cell layers were the result of extra cell divisions that originated in the root meristem (Figure 6A).

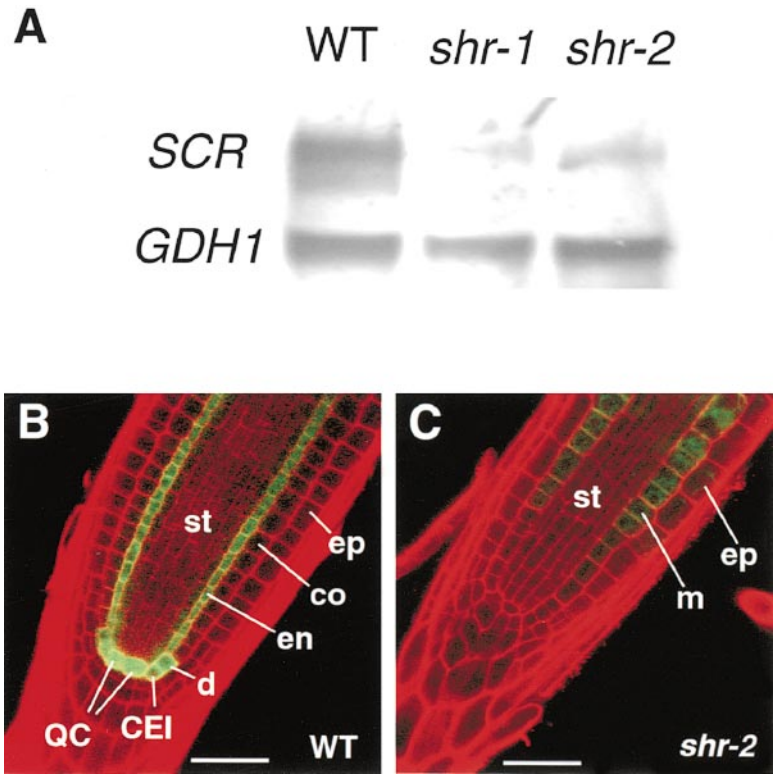

Figure 5. *SCR* Expression in *shr* Background

(A) *SCR* RNA accumulation in seedling roots. RNA blot analysis was performed with total RNA from 12-day-old wild-type, *shr-1*, and *shr-2* root tissues hybridized with a *SCR* gene-specific probe. The same blot was hybridized with a *GDH1* (Melo-Oliveira et al., 1996) gene-specific probe as a loading control.

(B and C) Expression of *SCR::GFP* in the primary root. GFP expression in (B) wild-type and (C) *shr-2* seedling roots harboring the *SCR::GFP* transgene indicating that the *shr* mutation results in reduced expression from the *SCR* promoter. Abbreviations as above. Bar, 50 μm.

To analyze the effects of ectopic *SHR* expression on cell specification, we used the JIM13 monoclonal antibody (Knox et al., 1990; Di Laurenzio et al., 1996) on root sections from *35S::SHR* seedlings. In wild-type the epitope recognized by the JIM13 antibody is found only on endodermis and some stele cells (Figure 7B). In the *35S::SHR* roots, the antibody bound to most of the supernumerary cells in addition to the stele and presumptive endodermis (Figure 6C).

To determine the spatial localization of *SHR* expression and its effect on *SCR* expression, we performed in situ hybridizations on root tissue from *35S::SHR* seedlings. As would be expected with expression driven by the 35S promoter, *SHR* RNA appeared to be in all tissues (except possibly in the external root cap cells) (Figure 6D). In the meristematic zone of wild-type roots, *SCR* is expressed very specifically in the endodermis (Di Laurenzio et al., 1996; Pysh et al., 1999). In the meristematic zone of *35S::SHR* roots, *SCR* expression appeared to be in all tissues except for the stele and the root cap (Figure 6E). The ectopic expression of *SCR* in the *35S::SHR* plants is consistent with our hypothesis that SHR is upstream of *SCR* in a pathway that leads to transcriptional activation of *SCR*. Taken together, these results indicate that ectopic *SHR* expression causes extra cell divisions and alters cell specification in the root meristem.

Cell Division and Cell Specification Are Uncoupled in Somatic Revertant Sectors

We used the genetic instability of the *shr-3* allele to investigate the relationship between *SCR* expression, ground tissue cell division, and cell specification. Infrequently, *shr-3* seedlings develop indeterminate primary or secondary roots. A relatively rare class of putative somatic sector roots are those with mutant cotyledons and an indeterminately growing primary root. These plants were used in our analysis because the embryonic origins of the primary root are well documented (Mayer et al., 1993).

SCR::GFP was crossed into the *shr-3* background, and seedlings with indeterminate primary roots and mutant cotyledons were visualized by confocal laser scanning microscopy. In all primary revertant roots, we observed a sector of wild-type ground tissue with GFP expression in the inner of the two layers (Figures 7G and 7H). This indicates that there is a partial restoration of the wild-type radial pattern. There was complete concordance of longer roots, sectors with divided ground tissue, and high-level GFP expression in the inner layer.

To determine the differentiation status of the primary revertant roots scored for *SCR::GFP* expression, transverse sections were analyzed for the presence of the epitope recognized by the JIM13 monoclonal antibody. In wild-type, the antibody decorates endodermis and some stele cells (Figures 7A and 7B), while in *shr*, antibody binding is restricted to the stele and is excluded from the mutant ground tissue layer (Figures 7C and 7D). In sections from partially revertant roots, the ground tissue cells that had divided always expressed this marker (Figures 7E and 7F). Occasionally, the continuous domain of divided cells was slightly broader than half of the root, although in most cases it was very narrow (data not shown). We also consistently detected ground tissue

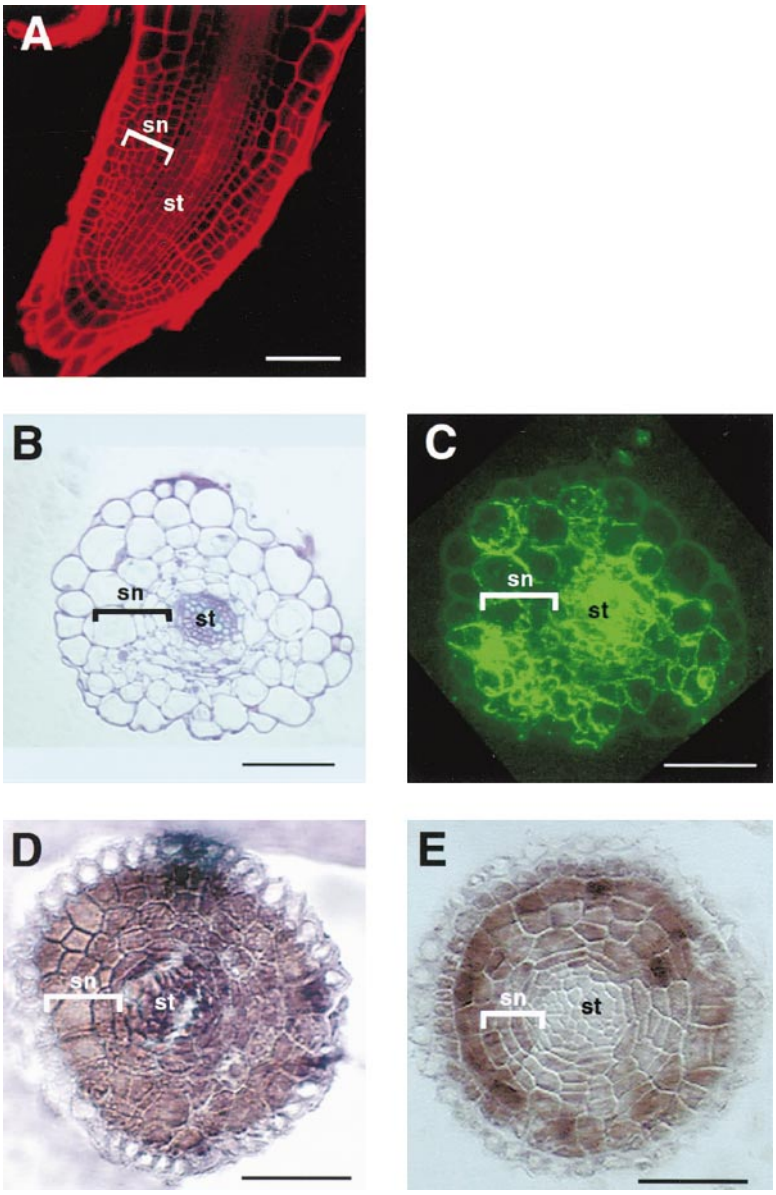

Figure 6. Effects of Ectopic Expression of *SHR*

(A) Confocal image of longitudinal optical section of root meristem of *35S*::*SHR* seedling. Note supernumerary cell files as compared to wild-type (Figure 5B).

(B) Transverse section of *35S*::*SHR* seedling root. Compare to wild-type transverse section (Figure 1C).

(C) Ectopic *SHR* expression results in altered cell specification as revealed by JIM13 antibody staining of cross-section of *35S*::*SHR* root (serial section of that shown in Figure 5B). Compare to wild-type JIM13 staining (Figure 7B) and *shr* JIM13 staining (Figure 7D).

(D) Expression of *SHR* in *35S*::*SHR* seedling analyzed by in situ hybridization on transverse root section with antisense *SHR* probe (compare to wild-type expression in Figure 3C).

(E) Expression of *SCR* in *35S*::*SHR* seedling analyzed by in situ hybridization on transverse root section with antisense *SCR* probe. In contrast to wild-type in which expression is restricted to the endodermis (Pysh et al., 1999), expression in *35S*::*SHR* is detected in all tissues except stele and root cap. Abbreviations as above except sn, supernumerary cell layers.

cells that had not divided (and did not express *SCR::GFP*) but were decorated by the antibody (cell with star in Figures 7E and 7F). This indicates that there has been a spatial uncoupling of cell division and cell specification resulting from the partial reversion process.

Discussion

SHR Is a Member of the GRAS Family of Putative Transcription Factors

The deduced amino acid sequence of *SHORT-ROOT* places it in the GRAS gene family, whose founding member is *SCARECROW* (Di Laurenzio et al., 1996; Pysh et al., 1999). Motifs including homopolymeric repeat regions, leucine heptad repeats, and putative nuclear localization signals found in all members of this family raised the possibility that they act as transcription factors. Nuclear localization of at least one member of the family (*RGA*) has been demonstrated (Silverstone et al., 1998). Moreover, it has been suggested that within the C terminus of some GRAS family proteins is a region similar to the SH2 domain of STAT proteins (Peng et al., 1999).

In addition to *SCR* and *SHR*, a third member of the GRAS family has been shown to be a possible regulator of radial patterning. The expression pattern of *SCL3* is restricted to the endodermis in the root (Pysh et al., 1999). This indicates that there is a subfamily of GRAS genes that participate in radial patterning. Another subfamily of GRAS genes that is involved in gibberellic acid signaling has been shown to share a conserved domain (Peng et al., 1997; Silverstone et al., 1998). No conserved domain that might be specific to GRAS genes involved in radial patterning was found in a comparison of SCR and SHR to other members of the family.

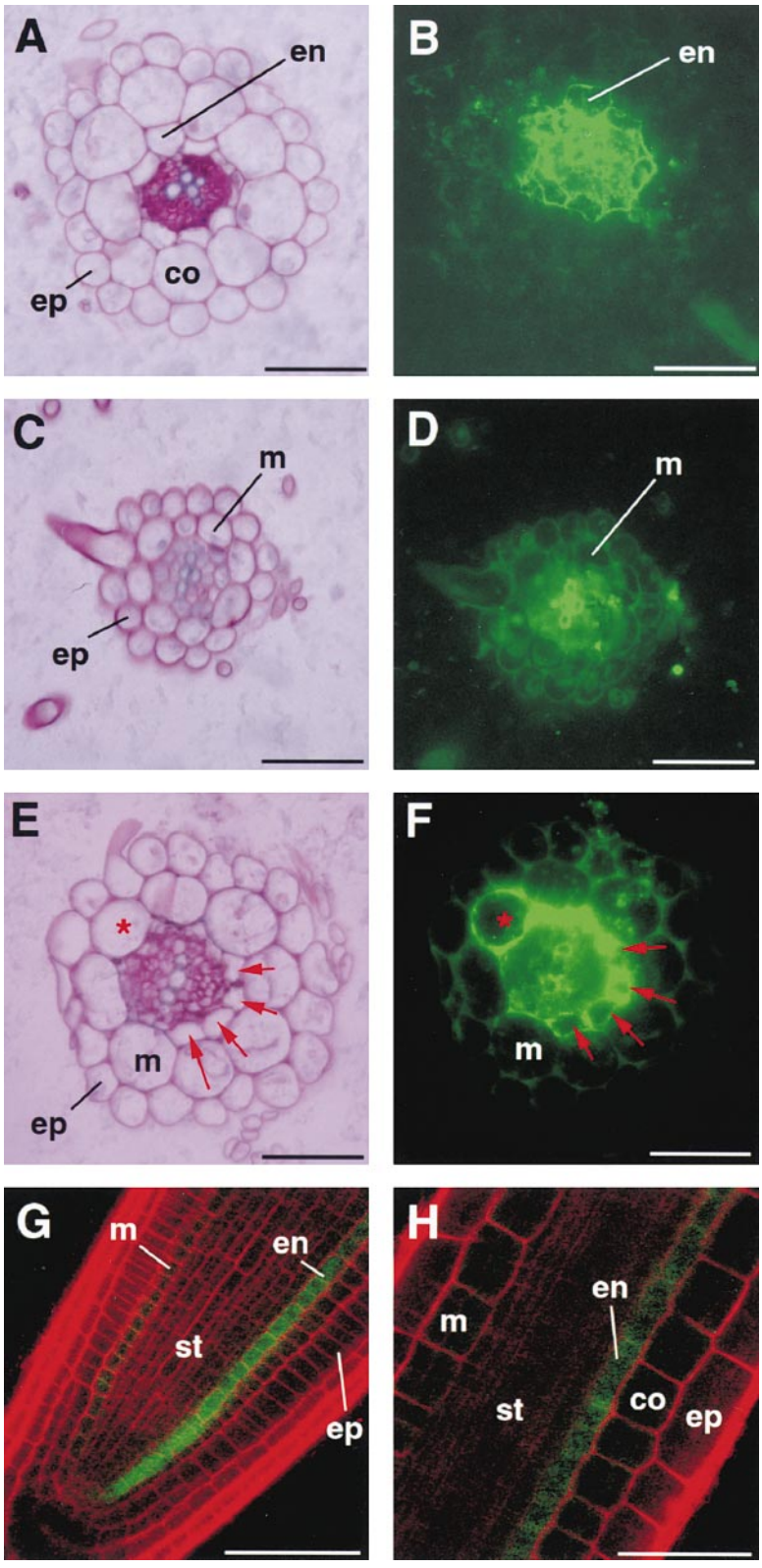

Figure 7. Primary Root Sector in the Unstable *shr-3* Allele

(A, C, and E) Transverse sections and (B, D, and F) JIM13 antibody staining (endodermis and stele marker) of primary roots. (A and B) wildtype; (C and D) *shr-3* (mutant phenotype); (E and F) *shr-3* with a primary root sector. (F) Red arrows indicate the divided ground tissue cells decorated by JIM13. The red star indicates an undivided ground tissue cell decorated by JIM13.

(G and H) Expression of the *SCR::GFP* reporter gene in the same *shr-3* seedling with the primary root sector shown in (E) and (F). Note that the *SCR::GFP* reporter gene is expressed strongly only in one cell file on the right side of the root, which corresponds to the divided cells seen in (E) and (F). Abbreviations as above. Bar, 50 μm.

SHR Is Upstream of SCR

Previously, we had shown that *shr* does not express endodermal markers in the root (Benfey et al., 1993; Scheres et al., 1995). The use of cortex markers revealed that the remaining ground tissue layer has differentiated attributes of cortex. From this, we can conclude that

SHR is required for both the asymmetric cell division that generates cortex and endodermis and for endodermal specification. Because *SCR* has been shown to primarily regulate the same asymmetric cell division, we hypothesized that *SHR* might function upstream of *SCR* in a common pathway. The epistasis of *shr* to *scr* was consistent with this hypothesis as was the downregulation of *SCR* RNA expression in a *shr* background.

Because SHR is a putative transcription factor, the simplest scenario was that SHR interacts directly with the *SCR* promoter. The expectation then was that *SHR* would be expressed in the precursor cells of the ground tissue. By in situ hybridization and promoter::marker gene expression, *SHR* expression is not detectable in the ground tissue lineage. Rather, it appears to be expressed exclusively in stele cells. Because the root radial pattern is established during embryogenesis, it was possible that *SHR* was first expressed in the embryonic ground tissue and then became restricted to stele tissue after germination. Our analysis of embryonic expression was not consistent with this hypothesis. On the contrary, *SHR* expression was found only in the precursors to the stele.

Expression of *SHR* in the stele suggested that it might play a role in development of this tissue. However, all cell types present in the wild-type stele appear to be present in *shr*, indicating that if there is an effect on the stele, it is subtle.

SHR Participates in Radial Signaling

The fact that SHR is required for ground tissue patterning and transcriptional regulation of *SCR* but is not expressed in ground tissue cells indicates that it may act in a non-cell autonomous manner. A trivial explanation would be that *SHR* expression in the ground tissue is just below detection limits. Analysis of revertant sectors in primary roots of the unstable *shr-3* allele that harbors the *SCR::GFP* construct was not consistent with this hypothesis. In these plants, we consistently found partial restoration of a two-layer ground tissue, with the inner layer expressing GFP and binding the JIM13 antibody. Moreover, we found ground tissue cells that had not divided and did not express GFP but did bind JIM13. Because we found this combination of marker expression in many roots, it is highly unlikely that this is due to multiple reversion events.

The simplest explanation of the partial reversion events, consistent with the fate map of *Arabidopsis* embryo, is that reversion results in *SHR* expression in a subset of stele cells. The first division in the embryo proper always occurs vertically before the horizontal divisions that separate the root and shoot poles (Mayer et al., 1993; Scheres et al., 1994). This would indicate that the excision event in plants with revertant roots and mutant cotyledons must have taken place after the first vertical division, which would result in, at most, reversion of half of the root tissue.

Due possibly to the small number of cells involved, we have been unable to determine the spatial domain of *SHR* expression by in situ hybridization in the sectored roots. Nevertheless, we can draw some conclusions based on the phenotype of the revertant roots. In the sectored roots, there are sharp boundaries between mutant ground tissue cells and apparently normal cortex and endodermal cells. This indicates that the presence of some *SHR*-expressing cells is not sufficient for complete rescue of the ground tissue, suggesting that the *SHR*-mediated signaling process is highly localized.

We can postulate two alternatives for the non-cell-autonomous regulation of *SCR* expression by SHR. First, it is possible that the SHR gene product is present only in the stele cells where it is expressed. In this scenario, SHR would regulate *SCR* expression through an intermediate that moves from the stele to the ground tissue cell lineage. Alternatively, the SHR protein itself might be transported via plasmodesmata from the stele to the ground tissue cell lineage. The latter scenario is supported by evidence that the maize knotted1 transcription factor can move from one cell lineage to another (Lucas et al., 1995).

The phenotype of *35S::SHR* roots supports our idea that SHR is a positive regulator of root radial patterning. The presence of supernumerary cell layers and altered cell specification in the extra cell layers strongly suggests that SHR is both necessary and sufficient for cell division and cell specification in the root meristem.

Three-Dimensional Cell Communication in the Root Meristem

Our results concerning the non-cell-autonomous mode of interaction of SHR with *SCR* provide insight into how positional information related to patterning is distributed in the plant meristem. Recently, the role of vascular tissue as a source of positional information has been demonstrated in the context of auxin signaling in organizing the distal pattern of the root (Sabatini et al., 1999). SHR-mediated radial patterning of the ground tissue provides further evidence for the role of vascular tissue as playing an important role in organizing plant organogenesis.

The manner by which the SHR-SCR pathway controls root radial patterning has at least superficial similarity to the regulation of cell fate in the shoot apical meristem by the *Arabidopsis WUSCHEL* (*WUS*) gene. WUS is a novel homeodomain protein that is required for the regulation of stem cell fate (Mayer et al., 1998) and acts in a regulatory feedback loop with the *CLAVATA* genes in the shoot apical meristem (Schoof et al., 2000). *WUS* expression is induced at an early stage of embryogenesis and is observed only in the cells underlying the presumptive shoot meristem but not in the presumptive shoot meristem, indicating that WUS acts in a non-cell-autonomous manner. Furthermore, there is a successive patterning process of the shoot meristem that involves asymmetric cell divisions marked by *WUS* mRNA accumulation (Mayer et al., 1998), in a manner analogous to the dynamic *SCR* expression pattern (Wysocka-Diller et al., 2000). Although the molecular action of SHR, SCR, and WUS is unknown, such a non-cell-autonomous regulation coupled to successive patterning appears to be a common process used in both the shoot and root meristems, the two stem cell populations in plants.

For the cortex/endodermal initial cell of the root meristem, van den Berg et al. (1995, 1997) have shown that a top-down signal is essential for the asymmetric division of its immediate daughter cell and that another contact-dependent signal from the underlying quiescent

center is essential for the maintenance of the undifferentiated status of the initial. We have now identified a radial signaling pathway that regulates the asymmetric division of the immediate daughter cell of the initial through the *SHR* and *SCR* genes. This indicates the presence of a three-dimensional signaling network, which controls the developmental status of the initial cell and its derivatives.

Experimental Procedures

Arabidopsis Strains and Growth Condition

shr-1 (in WS ecotype), *shr-2* (Col), and *scr-1* (WS) have been previously described (Benfey et al., 1993; Scheres et al., 1995; Di Laurenzio et al., 1996; Fukaki et al., 1998). Unstable *shr-3* and *shr-4* alleles (Col) were identified in lines containing the autonomous maize transposon, En (Wisman et al., 1998). The *SCR::GFP* line has been described previously (Sabatini et al., 1999; Wysocka-Diller et al., 2000). The growth condition of seedlings and plants has been described previously (Benfey et al., 1993).

Genetic Crosses

To determine allelism, a heterozygote carrying the *shr-2* allele was pollinated by *shr-3*. In the resulting progeny (n = 30), 34% showed the mutant phenotype indicating that the two mutations are allelic. The cross was confirmed by amplifying En specific sequences from the mutant plants (Wisman et al., 1998). A line homozygous for *shr-2* and *gl1* was pollinated by *shr-4*. In the resulting F1 progeny (n = 15), 100% showed the mutant phenotype indicating that the two mutations are allelic. The cross was confirmed by the presence of normal trichomes on the mutant.

To construct the *shr-1*, *shr-2*, and *shr-3* lines containing *SCR::GFP*, each *shr* allele was pollinated by a plant homozygous for the *SCR::GFP* fusion, and the resulting F1 and F2 plants were self-pollinated to generate F3 plants homozygous for both the fusion and the *shr* mutation. To construct the *shr-1* and *scr-3* lines containing *SHR::GFP*, each mutant line was pollinated by a plant heterozygous for a *SHR::GFP* fusion, and the resulting kanamycin-resistant F1 plants were self-pollinated to generate F2 plants that segregated lines homozygous for each mutation that contained the transgene.

Mapping

The following mapping crosses were performed: *shr-1*/Ws × Col, *shr-2*/Col × L*er*, and *shr-2*/Col × *ap2–10*/C24. In each case, homozygous wild-type or *ap2–10* plants were pollinated with *shr* pollen (with the exception of *shr-2*/Col × L*er* in which L*er* pollen was used to pollinate *shr-2*), and the resulting F1 plants were self-pollinated to generate F2 plants segregating the *shr* mutation. The rough map position of *shr-1* was obtained using SSLP (Bell and Ecker, 1994) and CAPS (Konieczny and Ausubel, 1993) markers by analyzing DNAs from 30 to 40 F2 *shr-1* mutant plants resulting from the mapping cross. For fine mapping, DNAs isolated from 74 and 56 F2 *shr* mutants resulting from crosses of *shr-1* and *shr-2* with wild-type, respectively, were analyzed for linkage to the marker nga1107 (Li and Chory, 1997). For the cross between *shr-2* and *ap2–10*, F2 plants carrying the recombinant chromosome were selected for kanamycin resistance conferred by the *NPT II* gene in the T-DNA linked to the *AP2* locus (Jofuku et al., 1994). After identification of the recombinant chromosomes, the order of *shr* in respect to the marker loci was determined by three-point analyses with flanking markers. Based on the analysis of 148, 112, and 486 chromosomes derived from the mapping crosses, 2, 4, and 1 recombination events were observed between *shr-1* and nga1107, *shr-2* and nga1107, and *shr-2* and *ap2*, respectively. The analysis of the recombinant chromosomes with flanking markers indicated that the *SHR* locus is on chromosome IV, between markers *ap2* (0.2 cM) and nga1107 (2.62 cM).

Cosegregation Analysis and Inverse PCR

Phenotypic mutants segregating among the progeny of a *shr-3* heterozygote were genotyped by Southern analysis. An end fragment (generated with oligos En7631 5′-GGCTCACATCATGCTAGTCC-3′ and En8183 5′-GTTGACCGACACTCTTAGCC-3′) of the En transposon was used to generate a probe. A band present in all mutants was identified in lanes corresponding to EcoRV-digested DNA (Figure 3A). A band with identical segregation pattern was observed with EcoRI digestion (data not shown). In this case, the fragment size was 2.6 kb, indicating that the plant-derived part of the sequence was about 200 bp.

The 2.6 kb EcoRI fragment was gel isolated, and inverse PCR was performed (as described by Long et al., 1993) using En sequences as a basis with primers 5′-TCTATACGAATAAGAGCGTCC-3′ (fwd) and 5′-TATTCGCGTCACAATAGTTCC-3′ (rev). An amplification product of approximately 500 bp was obtained, subcloned into a pCRII vector, and sequenced.

Sequence Analysis

Sequence of the amplified product was analyzed using the BLAST program (Altschul et al., 1990; Gish and States, 1993). It was identical to the end sequence of the BAC F18N2. The 2.8 kb ClaI-EcoRI end fragment containing the *SHR* gene was subcloned into pBluescript (Stratagene) and sequenced. Subsequently, the sequence was confirmed by the *Arabidopsis* Genomic Initiative analysis of chromosome IV (Mayer et al., 1999).

The *SHR* gene was amplified from the mutant lines using primers that had been designed based on the wild-type sequence. The *shr-2* allele contained an insertion sequence identical to a region from the BAC F21I17TRB (accession number, B24674).

Molecular Techniques

RNA gel blot analysis was performed essentially as described (Di Laurenzio et al., 1996). A 440 bp fragment representing a region of nonconserved coding region was used as a probe. This probe was also used to screen approximately 150,000 plaques of a cDNA library made from whole seedlings. RT-PCR was performed with M-MLV reverse transcriptase (Promega) on mRNA obtained separately from roots and shoots of 10-day-old seedlings. The two cDNA species and the amplification products from the RT-PCR were sequenced.

The *35S::SHR* construct was made by placing the coding region of *SHR* between the 35S promoter and the nopaline synthese polyadenylation sequence. The primers 5′-CAGTCGACTAGTCATATG GATACTCTCTTTAGATTA-3′ and 5′-TGTGGAATTGTGAGCCG-3′ were used to amplify a 2.8 kb subclone of the *SHR* genomic region as a template. The former primer removed an SpeI site at codon 7 of *SHR*, while creating new SpeI and NdeI sites around the first ATG. These mutations did not alter the encoded amino acid sequence. The latter primer was designed to anneal to downstream vector sequence in the template subclone. The PCR-amplified DNA fragment was cloned into pCR2.1 (Invitrogen) and sequenced. The SHR-coding region was excised as an SpeI fragment and inserted into the XbaI site of plasmid W104 (from Dr. T. Brears). The resulting plasmid was used to transform wild-type *Arabidopsis* plants (Col) by the floral dipping method (Clough and Bent, 1998).

Histochemical Techniques and In Situ Hybridization

Histochemical analysis using monoclonal antibodies (JIM13 and CCRC-M2) was performed as described (Di Laurenzio et al., 1996). For the construction of the *SHR* promoter::β-glucuronidase (GUS) marker gene line, the 2.5 kb region upstream of the *SHR* translational start site was PCR amplified using the primers 5′-CG***GGATCC***A GAAGCAGAGCGTGGGGTTTC-3′(fwd) and 5′-CG***GGATCC***TTTTAA TGAATAAGAAAATG-3′ (rev) (***GGATCC***; BamHI site). The 2.5 kb PCR fragment was inserted into pCR 2.1 using the TA cloning kit (Invitrogen), and, after BamHI digestion, it was subcloned into the BamHI site upstream of the GUS coding region in pBI101 (Clontech). This binary vector was used to generate transgenic plants as described above. T1 seeds were collected in separate pools, and transgenic plants were selected by planting on media containing kanamycin (50 μg/ml). GUS staining of the *SHR::GUS* line was performed as described (Malamy and Benfey, 1997). In situ hybridization analysis was performed as described in Di Laurenzio et al. (1996).

Imaging of GFP Expression

The 2.5 kb region upstream of the *SHR* translational start site was inserted directly upstream of the mGFP5-ER coding region in pBIN

(from J. Haseloff) and used to generate transgenic plants. For GFP analysis, roots were counterstained with 10 μg/ml propidium iodide (Sigma) and placed on slides in a drop of water. For analysis in embryos, embryo sacs were dissected from siliques and mounted in 50% glycerol in water. GFP fluorescence was imaged with a Leica confocal microscope, and the FITC channel (green: GFP) was overlaid onto the TRITC channel (red: autofluorescence and propidium iodide) to permit identification of the GFP-expressing cells.

Acknowledgments

We thank T. Nawy for help with RNA blot analysis and confocal microscopy, J. Lim for the initial mapping of the *SHR* locus, M. Starz for assistance with confocal microscopy, L. Pysh for in silico cloning of the BAC F18N2, N. Chen and H. Mundi for excellent technical assistance in genetic analyses, E. Wisman for the En-transposon lines, H. M. Lam and G. Coruzzi for the cDNA library, K. Roberts for the JIM13 antibody, M. Hahn for the CCRC-M2 antibody, J. Harada for the AX92 line, J. A. Hubbard for help with fluorescence microscopy, and B. Scheres, S. Small, M. Tasaka, and an anonymous reviewer for helpful comments on the manuscript. Y. H. was supported by a fellowship from the Academy of Finland and The Lewis B. and Dorothy Cullman Program for Molecular Systematic Studies, New York Botanical Garden; H. F. was supported by a fellowship from the Human Frontier Science Program (LT0112/98-M); J. W.-D. was supported by a postdoctoral fellowship from the National Institutes of Health; and K. N. was supported by a fellowship from the Japan Society for the Promotion of Science. This work was supported by a grant from the National Institutes of Health (R01-GM43778).

Received March 17, 2000; revised April 20, 2000.

References

Altschul, S.F., Gish, W., Miller, W., Myers, W.W., and Lipman, D.J. (1990). Basic local alignment tool. J. Mol. Biol. *215*, 403–410.

Bell, C.J., and Ecker, J.R. (1994). Assignment of 30 microsatellite loci to the linkage map of Arabidopsis. Genomics *18*, 137–144.

Benfey, P.N., Linstead, P.J., Roberts, K., Schiefelbein, J.W., Hauser, M-T., and Aeschbacher, R.A. (1993). Root development in Arabidopsis: four mutants with dramatically altered root morphogenesis. Development *119*, 57–70.

Clough, S.J., and Bent, A.F. (1998). Floral dip: a simplified method for *Agrobacterium*-mediated transformation of *Arabidopsis thaliana*. Plant J. *16*, 735–743.

Dietrich, R.A., Radke, S.E., and Harada, J.J. (1992). Downstream DNA sequences are required to activate a gene expressed in the root cortex of embryos and seedlings. Plant Cell *4*, 1371–1382.

Di Laurenzio, L., Wysocka-Diller, J., Malamy, J.E., Pysh, L., Helariutta, Y., Freshour, G., Hahn, M.G., Feldmann, K.A., and Benfey, P.N. (1996). The *SCARECROW* gene regulates an asymmetric cell division that is essential for generating the radial organization of the *Arabidopsis* root. Cell *86*, 423–433.

Freshour, G., Clay, R.P., Fuller, M.S., Albersheim, P., Darvill, A.G., and Hahn, M.G. (1996). Developmental and tissue-specific structural alterations of the cell wall polysaccharides of *Arabidopsis thaliana* roots. Plant Physiol. *110*, 1413–1429.

Fukaki, H., Wysocka-Diller, J., Kato, T., Fujisawa, H., Benfey, P.N., and Tasaka, M. (1998). Genetic evidence that the endodermis is essential for shoot gravitropism in *Arabidopsis thaliana*. Plant J. *14*, 425–430.

Gish, W., and States, D.J. (1993). Identification of protein coding regions by database similarity search. Nat. Genet. *3*, 266–271.

Jofuku, K.D., den Boer, B.G., van Montagu, M.V., and Okamuro, J.K. (1994). Control of Arabidopsis flower and seed development by the homeotic gene *APETALA2*. Plant Cell *6*, 1211–1225.

Haseloff, J., Siemering, K.R., Prasher, D.C., and Hodge, S. (1997). Removal of a cryptic intron and subcellular localization of green fluorescent protein are required to mark transgenic Arabidopsis plants brightly. Proc. Natl. Acad. Sci. USA *94*, 2122–2127.

Knox, J.P., Linstead, P.J., King, J., Cooper, C., and Roberts, K. (1990). Pectin esterification is spatially regulated both within cell walls and between developing tissues of root apices. Planta *181*, 512–521.

Konieczny, A., and Ausubel, F.M. (1993). A procedure for mapping *Arabidopsis* mutations using co-dominant ecotype-specific PCR-based markers, Plant J. *4*, 403–410.

Li, J., and Chory, J. (1997). A putative leucine-rich repeat receptor kinase involved in brassinosteroid signal transduction. Cell *90*, 929–938.

Long, D., Martin, M., Sundberg, E., Swinburne, J., Puangsomlee, P., and Coupland, G. (1993) The maize transposable element system *Ac/Ds* as a mutagen in Arabidopsis: identification of an *albino* mutation induced by *Ds* insertion. Proc. Natl. Acad. Sci. USA *90*, 10370–10374.

Lucas, W.J., Bouché-Pillon, S., Jackson, D.P, Nguyen, L., Baker, L., Ding, B., and Hake, S. (1995). Selective trafficking of KNOTTED1 homeodomain protein and its mRNA through plasmodesmata. Science *270*, 1980–1983.

Malamy, J.E., and Benfey, P.N. (1997). Organization and cell differentiation in lateral roots in *Arabidopsis thaliana*. Development *124*, 33–44.

Mayer, U., Buttner, G., and Jürgens, G. (1993). Apical-basal pattern formation in the Arabidopsis embryo: studies on the role of the gnom gene. Development *117*, 149–162.

Mayer, K.F.X., Schoof, H., Haecker, A., Lenhard, M., Jurgens, G., and Laux, T. (1998). Role of *WUSCHEL* in regulating stem cell fate in the Arabidopsis shoot meristem. Cell *95*, 805–815.

Mayer, K., Schuller, C., Wambutt, R., Murphy, G., Volckaert, G., Pohl, T., Dusterhoft, A., Stiekema, W., Entian, K.D., Terryn, N., et al. (1999). Sequence and analysis of chromosome 4 of the plant *Arabidopsis thaliana*. Nature *402*, 769–777.

Melo-Oliveira, R., Oliveira, I.C., and Coruzzi, G. (1996). Arabidopsis mutant analysis and gene regulation define a nonredundant role for glutamate dehydrogenase in nitrogen assimilation. Proc. Natl. Acad. Sci. USA *93*, 4718–4723.

Odell, J.T., Nagy, F., and Chua, N.-H. (1985). Identification of DNA-sequences required-for activity of the cauliflower mosaic virus-35S promoter. Nature *313*, 810–812.

Peng, J., Carol, P., Richards, D.E., King, K.E., Cowling, R.J., Murphy, G.P., and Harberd, N.P. (1997). The *Arabidopsis GAI* gene defines a signaling pathway that negatively regulates gibberellin responses. Genes Dev. *11*, 3194–3205.

Peng, J., Richards, D.E., Hartley, N.M., Murphy, G.P., Devos, K.M., Flimtham, J.E., Beales, J., Fish, L.J., Worland, A.J., Pelica, F., et al. (1999). "Green revolution" genes encode mutant gibberellin response modulators. Nature *400*, 256–261.

Pysh, L.D, Wysocka-Diller, J.W., Camilleri, C., Bouchez, D., and Benfey, P.N. (1999). The GRAS gene family in Arabidopsis: sequence characterization and basic expression analysis of the *SCARECROW-LIKE* gene. Plant J. *18*, 111–119.

Sabatini, S., Beis, D., Wolkenfelt, H., Murfett, J., Guilfoyle, T., Malamy, J., Benfey, P., Leyser, O., Bechtold, N., Weisbeek, P., et al. (1999). An auxin-dependent distal organizer of pattern and polarity in the *Arabidopsis* root. Cell *99*, 463–472.

Scheres, B., Wolkenfelt, H., Willemsen, V., Terlouw, M., Lawson, E., Dean, C., and Weisbeek, P. (1994). Embryonic origin of the *Arabidopsis* primary root and root meristem initials. Development *120*, 2475–2487.

Scheres, B., Di Laurenzio, L., Willemsen, V., Hauser, M.-T., Janmaat, K., Weisbeek, P., and Benfey, P.N. (1995). Mutations affecting the radial organisation of the *Arabidopsis* root display specific defects throughout the radial axis. Development *121*, 53–62.

Schoof, H., Lenhard, M., Haecker, A., Mayer, K.F.X., Jurgens, G., and Laux, T. (2000). The stem cell population of Arabidopsis shoot meristems is maintained by a regulatory loop between the *CLAVATA* and *WUSCHEL* genes. Cell *100*, 635–644.

Schumacher, K., Schmitt, T., Rossberg, M., Schmitz, G., and Theres, K. (1999). The *Lateral suppressor* (*Ls*) gene of tomato encodes a new member of the VHIID protein family. Proc. Natl. Acad. Sci. USA *96*, 290–295.

Silverstone, A.L., Ciampaglio, C.N., and Sun, T.-p. (1998). The *Arabidopsis RGA* gene encodes a transcriptional regulator repressing the gibberellin signal transduction pathway. Plant Cell *10*, 155–169.

van den Berg, C., Willemsen, V., Hage, W., Weisbeek, P., and Scheres, B. (1995). Cell fate in the *Arabidopsis* root meristem determined by directional signaling. Nature *378*, 62–65.

van den Berg, C., Willemsen, V., Hendriks, G., Weisbeek, P., and Scheres, B. (1997). Short-range control of cell differentiation in the *Arabidopsis* root meristem. Nature *390*, 287–289.

Wisman, E., Cardon, G.H., Fransz, P., and Saedler, H. (1998). The behaviour of the autonomous maize transposable element *En*/*Spm* in *Arabidopsis thaliana* allows efficient mutagenesis. Plant Mol. Biol. *37*, 989–999.

Wysocka-Diller, J.W., Helariutta, Y., Fukaki, H., Malamy, J.E., and Benfey, P.N. (2000). Molecular analysis of SCARECROW function reveals a radial patterning mechanism common to root and shoot. Development *127*, 593–603.

GenBank Accession Numbers

The *SHR* sequence has been deposited in GenBank under accession number AF233752. The sequence of the *shr-2* mutant allele that contains an insertion has been deposited under accession number AF233753.